10

Luminescence of intrinsic defects in the UV range of single crystals and ceramics based on yttrium-aluminum garnet

© K.N. Orekhova, M.V. Zamoryanskaya

Ioffe Institute, St. Petersburg, Russia

e-mail: orekhova.kseniia@gmail.com

Received March 18, 2025
Revised April 25, 2025
Accepted May 12, 2025

The luminescence of intrinsic defects of yttrium aluminum garnet in the ultraviolet range under electron beam irradiation is studied. The cathodoluminescence spectra of single crystals and ceramics based on yttrium aluminum garnet are obtained and interpreted. It is shown that the spectra of all samples consist of three luminescence bands, two of which are associated with Y_{Al}^{oct} antisite defects. It is noted that in ceramics the band associated with another type of point defect makes a greater contribution to luminescence than in single crystals

Keywords: yttrium aluminum garnet, cathodoluminescence, defects, antisite defects.

DOI: 10.61011/EOS.2025.07.61904.7699-25

Introduction

Materials based on yttrium aluminum garnet (YAG), activated by rare-earth ions (REI), find applications in various fields of science and technology. YAG single crystals are widely used as gain media in visible and infrared solid-state lasers [1,2], as scintillators, and as optical components. For all these applications, intrinsic and impurity defects are of great importance because they affect the optical properties of these materials. Studying intrinsic luminescence is also crucial for activated crystals, since the excitation mechanism of activators may include energy transfer from high-energy levels of intrinsic defects to luminescent centers [3]. This is especially important when developing scintillators.

The nature of intrinsic luminescence bands in YAG single crystals has been discussed for over 40 years. It is assumed that UV luminescence in YAG is caused by the presence of antisite defects (AD). In garnet-type crystals, antisite defects are common [4,5]; they represent the substitution of one type of atom by another in the crystal lattice site. Such defects arise due to the presence of two equally charged cations Y^{3+} and Al^{3+} and the high temperature during crystal growth, which causes thermodynamic disorder in the lattice. ADs, like any point defects, increase the crystal's entropy because their formation requires certain energy. Most of the energy for forming a point defect is associated with the disruption of atomic periodicity and bonding forces between atoms. Since the YAG structure has two different Al atomic positions, several types of ADs can form in the cation sublattice: an Al ion in the dodecahedral Y position (AlY^{dod}) and an Y ion in the tetrahedral (Y_{Al}^{tet}) or octahedral (Y_{Al}^{oct}) positions of Al. According to the literature, the most common AD in YAG is Y_{Al}^{oct} [5]. The study [6] showed that ADs have the lowest formation energy in YAG, and the Y_{Al}^{oct}AD is energetically more favorable than other ADs. The probability of formation of this defect type increases with synthesis temperature. Since ceramics are synthesized at much lower temperatures than single crystals, it can be assumed that ADs of the Y_{Al}^{oct} type and luminescence associated with such defects are absent in ceramics.

Both single crystals and ceramics based on YAG are of great practical interest. Oxide nano- and micro-ceramics activated by REI [7–11] are developed as alternatives to single crystals because they have several advantages — faster and simpler production technology, the ability to create large optical materials with controlled doping profiles that are difficult to obtain as single crystals, and uniform activator distribution.

The first reports on the successful synthesis of transparent laser ceramic based on YAG:Nd, comparable in specific laser generation power to commercial single crystals, were presented in [12]. Subsequent studies showed that to achieve high ceramic transparency, the thickness of grain boundaries should not exceed ~ 1 nm and the material should be free of intergranular pores and impurity phases [13,14].

Since ceramics contain a large number of grain boundaries (interfaces), their influence on luminescent properties must be studied. Currently, the energetic structure of oxide ceramics is insufficiently explored. Due to the influence of energy levels associated with interfaces and grain boundaries on luminescence mechanisms, the optical properties of polycrystals may change. For example, the work [15] showed different luminescence kinetics of activators in YAG-based ceramics, related to the presence of grain boundaries and interfaces.

Intrinsic defect luminescence in undoped yttrium aluminum garnet crystals is observed in the UV and blue spectral ranges. The excitation of such luminescence occurs within the intrinsic absorption band region (above 7 eV) [16,17], which makes classical photoluminescence excitation techniques (up to 6 eV) unsuitable for these studies. To excite intrinsic defect luminescence, it is optimal

to use a high-energy excitation of optical emission, for example, irradiation with an electron beam of medium energies (1−40 keV).

The main objective of this work is to study the spectra of intrinsic defects in the UV range in YAG single crystals and ceramics using local cathodoluminescence.

Samples and Research Methods

As part of this work, a series of YAG single crystal (SC) and ceramic samples activated with various dopants, obtained by different methods, were investigated. Ceramics produced by different techniques (nanoceramics, NANO, and microceramics, MICRO) and single crystal samples grown by the horizontal direct technique were studied.

YAG:Nd and YAG:Eu nanoceramic samples were synthesized from nanopowders by low-temperature high-pressure sintering (LTHP) at the Institute of Low Temperature and Structural Research (Wrocesaw, Poland) [18]. Nanocrystalline powders of YAG:Nd (1 mol%) and YAG:Eu (1 mol%) were obtained by a modified Pechini method. The average grain size of the initial nanopowders was about 50 nm. Tablets of 5 mm diameter were formed by cold pressing at 50 MPa. The tablets were placed in a toroidal-type container and pressed at 8 GPa and 450 °C for 1 min.

A microceramic sample of YAG:Nd was synthesized by the reactive solid-state sintering method described in [19] at the V.A. Kotelnikov Institute of Radio Engineering and Electronics. The YAG micropowders were uniaxially pressed at 50 MPa. The compacts were then isostatically pressed at 250 MPa and sintered in vacuum at 1650 °C. The heating rate was about 0.3 °C/min. After sintering, the sample was additionally annealed in air at 1100 °C for 32 h.

YAG, YAG:Nd and YAG:Eu single crystals were synthesized by the horizontal direct technique [20] at the Vavilov State Optical Institute at 1930 °C.

Structural studies of the nanoceramic and microceramic YAG:Nd samples were performed using a LYRA 3 FEG scanning electron microscope (TESCAN, Czech Republic). The samples were investigated by scanning electron microscopy (SEM) and electron backscatter diffraction (EBSD) at accelerating voltages of 10 and 15 kV with variable beam currents (500 pA−1 nA). For EBSD analysis of the YAG:Nd microceramic sample, the surface was ion-polished using the SEMPrep2 ion milling system (Technoorg-Linda Co Ltd, Hungary) under the following conditions: ion accelerating voltage Ar^+ 10 kV, milling time 1 h.

Cathodoluminescence (CL) studies were carried out on a UV-range optical spectrometer of original design [21], attached to a Camebax electron probe microanalyzer (France). Electron beam parameters were: accelerating voltage 20 kV, current 50 nA, diameter 2 μm. The spectral resolution was 0.5 nm.

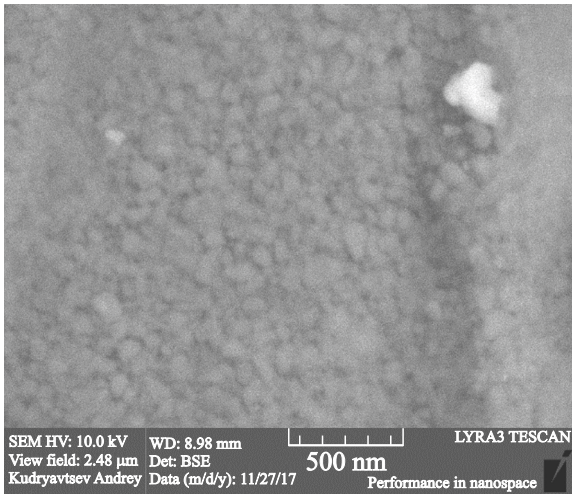

Figure 1. SEM image of a YAG:Eu nanoceramic sample.

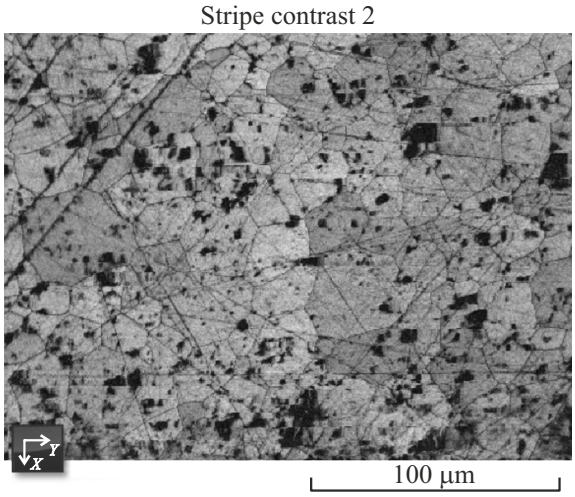

Figure 2. SEM image of the surface area of the YAG:Nd microceramic sample after EBSD data processing. Areas without electron diffraction (contaminations, scratches) are shown in black.

Experimental Results

SEM and EBSD

Figure 1 presents a characteristic SEM image of the YAG:Eu nanoceramic sample, from which the grain size can be estimated. After image processing, the average grain size in the samples was found to be about 50 ± 10 nm. Results on grain size and grain size distribution of the nanoceramics are reported in [13].

The grain boundaries of the YAG:Nd microceramic in Fig. 2 are highlighted according to the different grain orientations obtained from the EBSD analysis (Fig. 3). Different colors in Fig. 3 indicate different grain orientations relative to the selected direction (in this case — relative to the sample surface normal). The RGB channels correspond to three selected crystallographic directions of the crystal

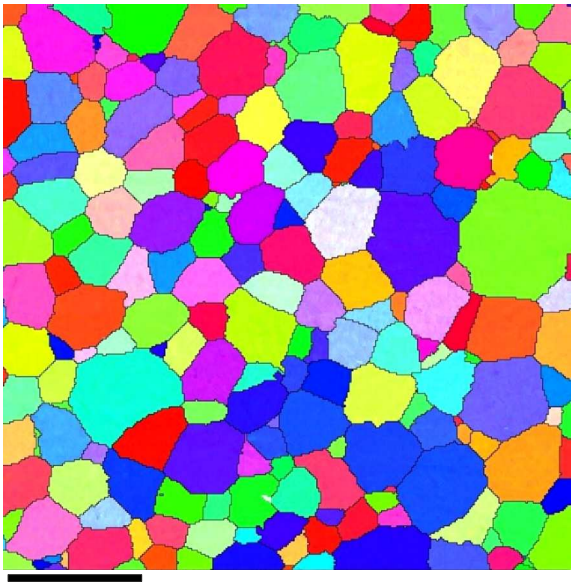

Figure 3. Orientation map of the YAG:Nd microceramic sample area.

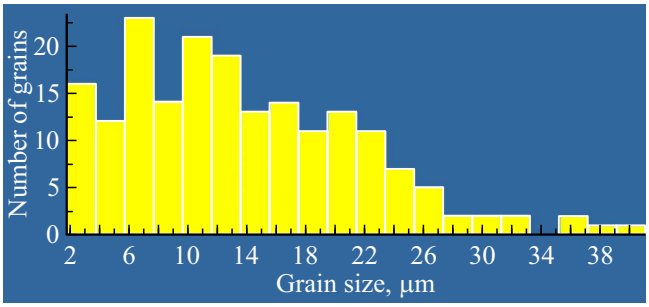

Figure 4. Average grain size in the YAG:Nd microceramic sample.

lattice. The color of a grain uniquely identifies its orientation relative to the chosen direction.

Figure 4 shows the distribution of equivalent circle diameters corresponding to the average grain sizes in the YAG:Nd microceramic sample. According to the results, the average grain size varies from a few to several tens of micrometers.

Cathodoluminescence Spectra and Their Interpretation

CL of YAG intrinsic defects was obtained at $T = 77$ K. The CL intensity of intrinsic defects was of the same order for all samples. Figure 5 shows the normalized CL spectra of the samples in the UV range.

In YAG:Nd samples, bands referred to transitions from the $^2F(2)_{5/2}$ level of neodymium ions (Nd^{3+}) overlap with the intrinsic YAG luminescence. Literature data indicate that intrinsic luminescence in the UV range consists of a superposition of three broad bands, so the measured CL spectra were decomposed into three bands. The CL

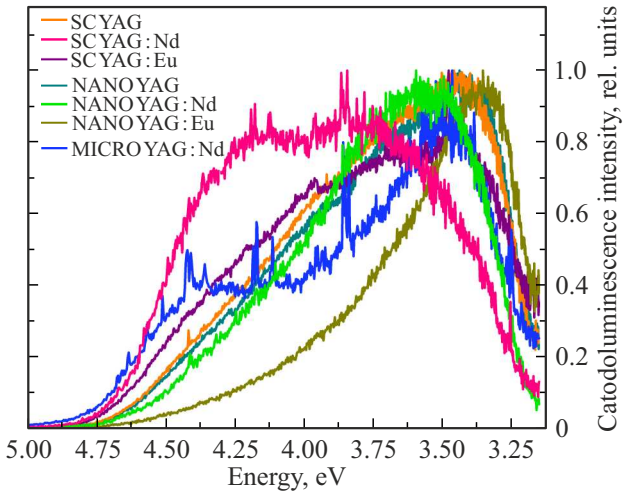

Figure 5. CL spectra of samples in the UV range at $T = 77$ K.

band decomposition into Gaussian curves was performed using *Origin* software. Fig. 6, *a*–*f* shows examples of the CL spectrum decomposition for all samples. The table presents the results of the intrinsic luminescence band decomposition. As seen, the positions of the CL bands for YAG-based samples coincide within error margins. The main contribution to UV luminescence comes from the band with a maximum at 3.7–3.8 eV. According to the literature, this band is related to luminescence of Y_{Al}^{oct} — antisite defects — Y ions occupying octahedral positions of Al instead of their regular dodecahedral sites [22]. The high-energy luminescence band (4.3–4.4 eV) is associated with exciton luminescence localized near Y_{Al}^{oct} ADs [23]. Various works report the maximum position of this band from 4.2 eV at 300 K to 4.95 eV at 5 K (references [3–8] in [24]). Relatively little is known from the literature about the luminescence band with a maximum at 3.4 eV. In work [25], this luminescence band was observed in commercial YAG:Ce samples and had no unambiguous interpretation. Literature indicates that the intrinsic luminescence band with a maximum near 3.3–3.4 eV is most intense in YAG samples containing high defect concentrations, particularly ceramics. However, the specific defect types are not identified by authors.

Thus, intrinsic luminescence of YAG single crystals and ceramics in the UV range does not differ fundamentally. However, in ceramic samples, the band with the 3.4 eV maximum contributes more significantly to luminescence than in single crystals. This suggests a higher defect concentration in ceramics, possibly related to the increased number of interfaces. This hypothesis requires further investigation.

Conclusion

Luminescence bands related to antisite defects — Y_{Al}^{oct} are observed in the spectra of YAG single crystals and ce-

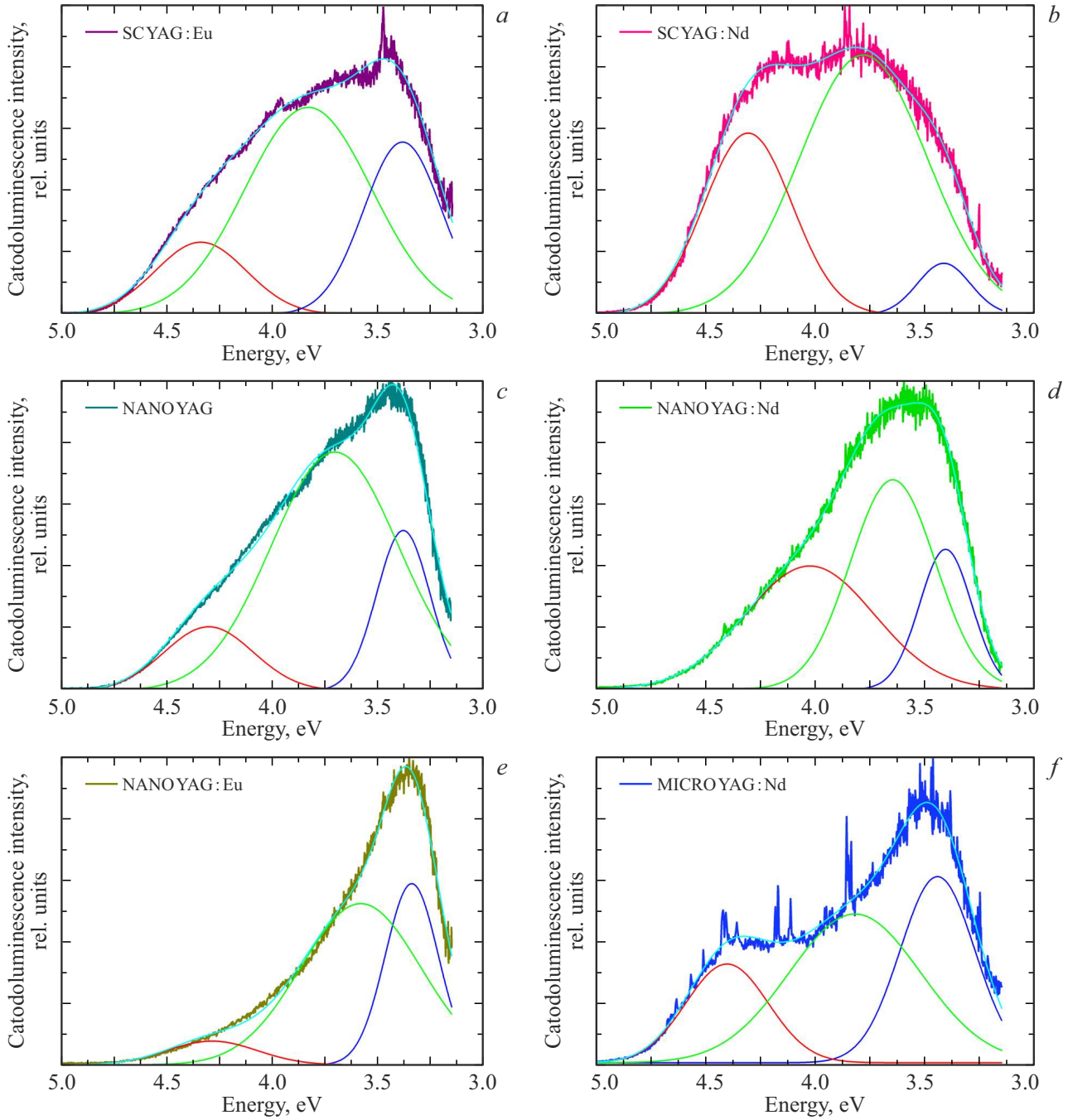

Figure 6. Examples of intrinsic CL band decomposition of samples: (*a*) SC YAGEu; (*b*) SC YAGNd; (*c*) NANO YAG; (*d*) NANO YAGNd; (*e*) NANO YAGEu; (*f*) MICRO YAGNd.

ramics. Additionally, a band not previously described in the literature is observed, which is interpreted as related to a higher defect concentration and possible uncontrolled impurities. It is shown that this band contributes more significantly in ceramic CL spectra than in single crystals. The study of defect luminescence is extremely important for the development of new scintillators and phosphors, as these defects can serve as energy donors for activator excitation.

Acknowledgment

The authors thank Ph.D. A. Kudryavtsev from the demonstration laboratory of TESCAN LLC (Saint Petersburg, Russia) for assistance with SEM and EBSD studies.

This research was supported by the Russian Science Foundation grant N 24-72-00112, https://rscf.ru/project/24-72-00112/. № 24-72-00112, https://rscf.ru/project/24-72-00112/.

Results of intrinsic CL band decomposition for various samples

Sample	Position, eV	Error, eV	FWHM, eV	Error, eV Relative	error integral intensity, %	
SC	3.4	0.01	0.3	0.05	20	10
(*single crystal*)	3.8	0.02	0.6	0.01	55	10
	4.3	0.02	0.5	0.06	25	5
NANO	3.4	0.05	0.3	0.01	25	5
(*nanoceramics*)	3.7	0.06	0.6	0.04	65	5
	4.3	0.02	0.4	0.02	10	2
MICRO	3.4	0.02	0.3	0.00	35	5
(*microceramics*)	3.8	0.02	0.6	0.00	45	5
	4.4	0.06	0.4	0.00	20	5

Conflict of interest

The authors declare that they have no conflict of interest.

References

[1] G.F. Albrecht, S.A. Payne. Solid-state Lasers. *Electro-Optics Handbook*. ed. by R.W. Waynant, M.N. Ediger, 2nd ed. (Professional Publishing, N.Y., 2000), ch. 5.

[2] A.A. Kaminskij, B.V. Mill', S.E. Sarkisov. it Fizika i spektroskopiya lazernyh kristallov (Nauka, M., 1986). (in Russian)

[3] K. Orekhova, R. Tomala, M. Zamoryanskaya. J. Alloy. Compd., **858**, 157731 (2021). DOI: 10.1016/j.jallcom.2020.157731

[4] M. Nikl, E. Mihokova, J. Pejchal, A. Vedda, Yu. Zorenko, K. Nejezchleb. Phys. Stat. Sol. (b), **242**, R119–R121 (2005). DOI: 10.1002/pssb.200541225

[5] M.K. Ashurov, Y. Voronko, V.V. Osiko, A.A. Sobol, M.I. Timoshechkin. Phys. Stat. Sol. (a), 42(1), 101-110 (1977). DOI: 10.1002/pssa.2210420108

[6] Z. Li, B. Liu, J. Wang, L. Sun, J. Wang, Y. Zhou. J. Am. Ceram. Soc., **95** (11), 3628–3633 (2012). DOI: 10.1111/j.1551-2916.2012.05440.x

[7] R. Tomala, L. Marciniak, J. Li, Y. Pan, K. Lenczewska, W. Strek, D. Hreniak. Opt. Mater., **50**, 59–64 (2015). DOI: 10.1016/j.optmat.2015.06.042

[8] A.A. Kaminskii, V.V. Balashov, E.A. Cheshev, Y.L. Kopylov, A.L. Koromyslov, O.N. Krokhin, V.B. Kravchenko, K..V. Lopukhin, V.V. Shemet, I.M. Tupitsyn. J. Phys.: Conf. Ser., **740** 012009 (2016). DOI: 10.1088/1742-6596/740/1/012009

[9] M. Pokhrel, N. Ray, G.A. Kumar, D.K. Sardar. Opt. Mater. Express., **2** (3), 235–249 (2012). DOI: 10.1364/OME.2.000235

[10] J. Zhou, W. Zhang, T. Huang, L. Wang, J. Li, W. Liu, B. Jiang, Y. Pan, J. Guo. Ceram. Int., **37** (2), 513–519 (2011). DOI: 10.1016/j.ceramint.2010.09.031

[11] I.O. Vorona, R.P. Yavetskiy, M.V. Dobrotvorskaya, A.G. Doroshenko, S.V. Parkhomenko, A.V. Tolmachev, D. Yu. Kosyanov, L. Gheorghe, C. Gheorghe, S. Hau, M. Enculescu. Opt. Mater., **77**, 221-225 (2018). DOI: 10.1016/j.optmat.2018.01.038

[12] A. Ikesue, T. Kinoshita, K. Kamata, K. Yoshida. J. Am. Ceram. Soc., **78** (4), 1033–1040 (1995). DOI: 10.1111/j.1151-2916.1995.tb08433.x

[13] A. Ikesue, Y.L. Aung, T. Taira, T. Kamimura, K. Yoshida, G.L. Messing. Annu. Rev. Mater. Res., **36** (1), 397–429 (2006). DOI: 10.1146/annurev.matsci.36.011205.152926

[14] S. Kochawattana, A. Stevenson, S.-H. Lee, M. Ramirez, V. Gopalan, J. Dumm, V.K. Castillo, G.J. Quarles, G.L. Messing, J. European Ceram., **28** (7), 1527–1534 (2008). DOI: 10.1016/j.jeurceramsoc.2007.12.006

[15] K. Orekhova, M. Zamoryanskaya. J. Lumin., **251**, 119228 (2022). DOI: /10.1016/j.jlumin.2022.119228

[16] G.A. Slack, D.W. Oliver, R.M. Chrenko, S. Roberts. Physical Review, Phys. Rev., **177** (3), 1308 (1969). DOI: 10.1103/PhysRev.177.1308

[17] V.N. Kolobanov, V.V. Mihajlin, N.N. Petrovnin, D.A. Spasskij, Yu.V. Zorenko. Vestn. Mosk. hboxun-ta. Ser. 3. Fiz. Astron., bf 1, 35–37 (2007). (in Russian)

[18] R. Fedyk, D. Hreniak, W. Łojkowski, W. Stręk, H. Matysiak, E. Grzanka, S. Gierlotka, P. Mazur. Opt. Mater., **29** (10), 1252–1257 (2007). DOI: 10.1016/j.optmat.2006.05.016

[19] A.A. Kaminskii, V.V. Balashov, E.A. Cheshev, Yu.L. Kopylov, A.L. Koromyslov, O.N. Krokhin, V.B. Kravchenko, K.V. Lopukhin, V.V. Shemet. Opt. Mater., **71**, 103–108 (2017). DOI: 10.1016/j.optmat.2016.05.015

[20] H.S. Bagdasarov, N.B. Bolotina, V.I. Kalinin, V.F. Karyagin, B.V. Kuz'min, L.A. Muradyan, S.N. Ryadnov, E.M. Uyukin, T.S. Chernaya, E.A. Fedorov, V.S. Chudakov, V.I. Simonov. Kristallografiya, **36** (3) 715–728 (1991). (in Russian)

[21] M.V. Zamoryanskaya, S.G. Konnikov, A.N. Zamoryanskij. Prib. tekh. eksperim., **4**, 62–69 (2004). (in Russian) DOI: 10.1023/B:INET.0000038392.08043.d6

[22] Yu. Zorenko, E. Zych, A. Voloshinovskii. Opt. Mater., **31** (12), 1845–1848 (2009). DOI: 10.1016/j.optmat.2008.11.026

[23] Yu. Zorenko, A. Voloshinovskii, V. Savchyn, T. Voznyak, M. Nikl, K. Nejezchleb, V. Mikhailin, V. Kolobanov, D. Spassky. Phys. Stat. Sol. (b), **244** (6), 2180–2189 (2007). DOI: 10.1002/pssb.200642431
[24] V. Babin, K. Blazek, A. Krasnikov, K. Nejezchleb, M. Nikl, T. Savikhina, S. Zazubovich. Phys. Stat. Sol. (c), **2** (1), 97–100 (2005). DOI: 10.1002/pssc.200460120
[25] V.M. Lisitsyn, V.A. Vaganov, L.A. Lisitsyna, Zh.T. Karipbayev, M. Kemere, A.T. Tulegenova, Y. Ju, Y.N. Panchenko. Russ. Phys. J., **63**, 1003–1009 (2020). DOI: 10.1007/s11182-020-02130-3

Translated by J.Savelyeva